

# Acoustic Real-time Sensor for Ingestive Behaviour of Grazing Cattle

Luciano S. Martínez Rau\*<sup>1</sup>, Nestor N. Deniz<sup>1</sup>, José O. Chelotti<sup>1</sup>,  
Leonardo L. Giovanini<sup>1</sup>, and Pablo A. Kler<sup>2</sup>

5 <sup>1</sup>Research Institute for Signals, Systems and Computational  
Intelligence, sinc(i)

<sup>2</sup>Research Center for Computational Methods

## Abstract

10 The increment of food market requirements and competitiveness  
makes that industry needs more accurate sensing and monitoring tools.  
Due to the large temporal dynamics necessary to monitor some animal  
behaviours, the autonomy and storage capacity of the devices  
involved becomes critical. In this work, we introduce a device specifically  
15 developed for on-line monitoring, quantifying and recording the  
feeding patterns of dairy cows. The prototype consists of an embedded  
circuit that records and analyzes the sounds produced by the animal  
to detect, classify and quantify the events related with the feeding  
behaviour. It implements an algorithm recently developed, which  
20 was adapted for its execution in a microcontroller based embedded  
system. A microcontroller with power management technology, combined  
with high efficiency harvesting power supply and power management  
firmware, enable long-term operation. The technology presented  
within this publication is protected under international patent applica-  
tion PCT/IB2016/057627.

## 25 1 Introduction

Despite the large number of successful applications, the livestock sector shows  
a lack of Wireless sensor solutions for monitoring the feeding behaviour. This

---

\*Corresponding author. lmrau@sinc.edu.unl.ar

situation can be understood from the stringent operational requirements that devices must satisfy to fulfill this task. In this sense, a device for monitoring the feeding behaviour of cattle must be: *i*) **Portable** in order not to interfere with the natural behaviour of the animal; *ii*) **Real-time processing** to allow continuous monitoring and reduce the communication and memory requirements; *iii*) **Autonomous operation** and **long operating time** to allow the recording and analysis of long term behaviours in the grassland (pasture); and *vi*) **Robustness** to operate in the environmental conditions imposed by outdoor activities.

A major requirements is that the sensors can operate automatically and autonomously for long period of time. However, to obtain a sensor with such characteristics it should be used a scheme of energy harvesting and a wireless technology to transmit the data frames to a personal computer (PC). In fact, in spite of the recent sensors on recording data for free-grazing cattle (see [1, 2]), up to this date to the best of our knowledge, there is no sensor capable of analyzing in real-time the acoustic emission produced by ruminants during their feeding activities.

One of the most accepted ways to perform monitoring of ruminant feeding is through the detection, classification and quantification of the three most common events of grazing activity: chew, bite, and composed chew-bite [3]. The importance of being able to determine these events is related to the quality and quantity of the food ingested by the animal [4]. However, currently available sensors are only able to detect jaw movement, behaviour detection (eating, ruminating, other) or to distinguish between chew and bite grazing event, and is unable to recognize the chew-bite event [5]. The first attempts for developing acoustic emission based algorithms for the detection and classification of these events are recent [6, 7].

The novel contribution of this paper includes a real-time sensor for ingestive behaviour monitoring of grazing cattle by means of acoustic emission analysis. Moreover, this paper introduces an acoustic emission sensing technique based on the algorithm developed by Chelotti et al. [6], embedded in the sensor for detection and classification of ingestive events. This is the first time acoustic emission sensing and processing, wireless communication, and energy harvesting, converge in a unique sensor solution for feeding behaviour analysis.

## 2 Sensing Principle

The proposed on-site real-time data processing and evaluation algorithm aims to detect the feeding activities of ruminants. When a ruminant is feeding,

it moves the jaw to perform two activities: *biting* (**B**), when forage is apprehended and cut, and *chewing* (**C**), when forage is crushed to reduce the size of the particles and increase the surface/volume ratio. The combined motion, *chewbite* (**CB**), is the combination of the both movement. Then, the feeding behaviour can be categorized in terms of a temporal sequence of **B**, **C**, and **CB** [7].

Based on the shape, intensity and duration of the time-domain envelope of the these three characteristic signatures (**C**, **B**, and **CB**), Chelotti et al. [6] developed and evaluated an algorithm able to detect and classify the ingestive events in real-time. Fig. 1 shows a diagram of the algorithm. The algorithm was divided into two sequential tasks: *detection and segmentation* and *classification*. These tasks can be thought as a set of successive stages [Fig. 1].

After digitalizing the acoustic monitoring, the resulting signal is conditioned by removing the tendencies present in the signal. This task is performed using an adaptive least-mean square filter. Once the trend and noises have been removed, two signals are computed from  $S(k)$ : (i) the signal envelope  $S_E(k)$  which is computed by filtering the absolute value of  $S(k)$ ; and (ii) the peak amplitude  $S_M(k)$  which is determined as the maximum value in a sliding window of 100 samples.  $S_E(k)$  and  $S_M(k)$  are then subsampled to 100 S/s, generating  $S_E(k^*)$  and  $S_M(k^*)$  in order to decrease the computational and memory requirements.

The next steps are the detection and classification of the events. This is performed by comparing  $S_E(k^*)$  with a time-varying threshold  $T(k^*)$ , which is generated online. If an event is detected (i.e.  $S_E(k^*) > T(k^*)$ ), the algorithm proceeds to compute the acoustic monitoring time-domain features (shape, duration, and maximum amplitude) in a window centered at the sample in which the event was detected. Then, the classifier proceeds to label the event using the extracted features. Finally, once the event is classified, the system estimates the characteristic parameters of the event (period, maximum amplitude, energy, among others). The period and energy content of the event are computed from  $S_E(k^*)$ , while the maximum amplitude  $S_M(k^*)$  is computed from the sound  $S(k)$ . For further details about the algorithm, see [6]. Once a potential event is detected, the algorithm computes the features of the envelope and then the event classifier labels the event. The features are gathered with other relevant information in an information package (see section 3.3).

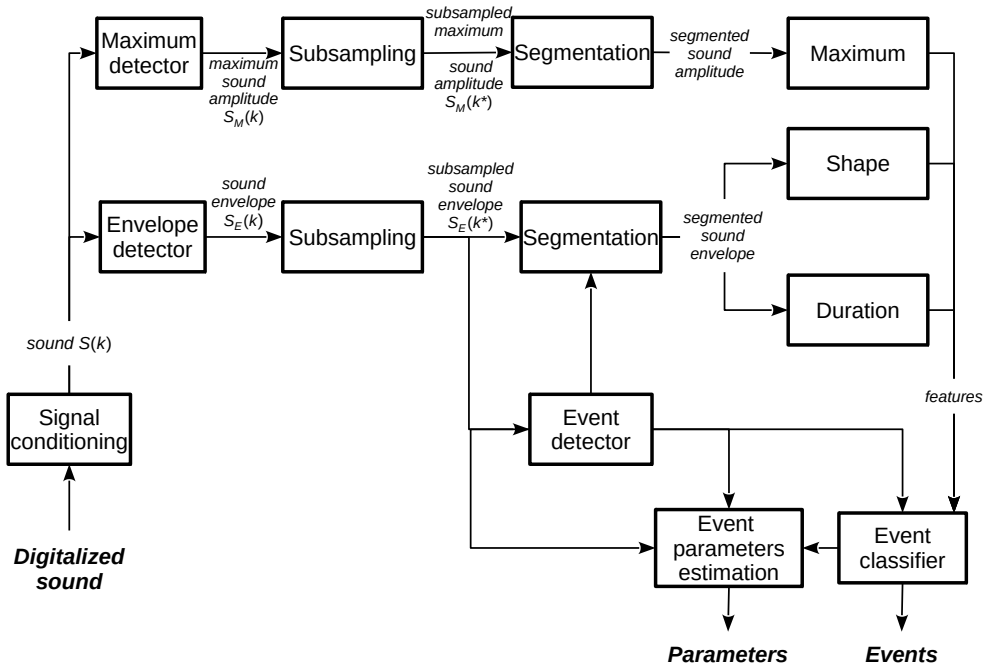


Figure 1: Diagram of the algorithm for ingestive event detection and classification.

### 3 Embedded system architecture and management

105 The design of a battery-powered embedded system requires a detailed analysis of each subsystem in order to minimize size, cost, and, principally power consumption. The Sensor Unit Device (SUD) has been designed as a trade-off between minimizing power consumption and parameter estimation accuracy. The SUD comprises different interconnected modules as shown in  
 110 Fig. 2. All the modules have been designed to efficiently use the power available in the device while providing the best performance. The final resulting packaged SUD is shown in Fig. 3. The SUD is located on the neck of the animal, just behind the head. The embedded device was built around an  
 115 MCF51JM128 (NXP Semiconductors, Eindhoven, Netherlands) microcontroller unit (MCU).

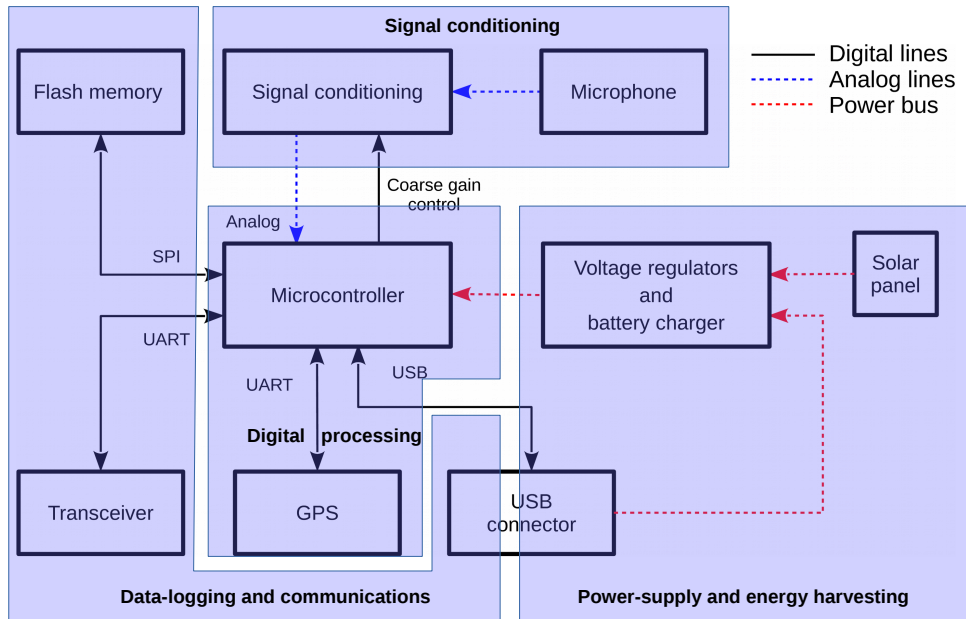


Figure 2: Block diagram of the embedded system.

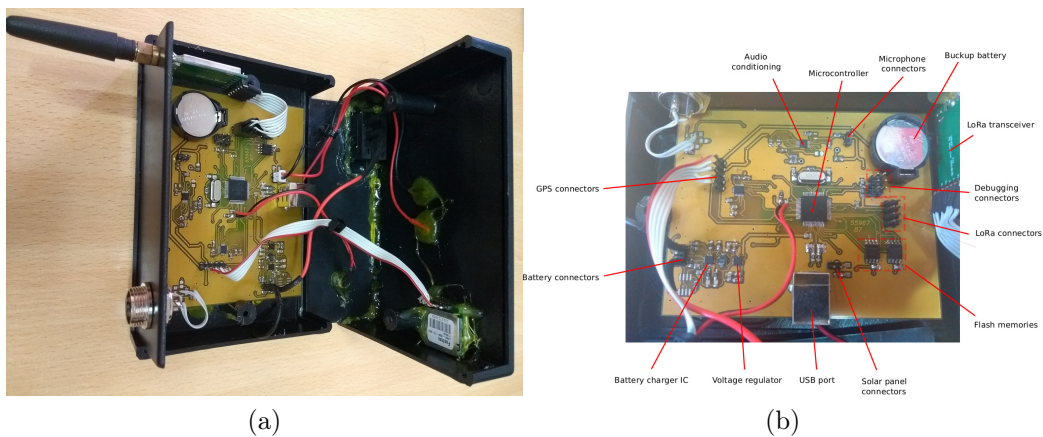


Figure 3: Printed circuit board design of the embedded system.

### 3.1 Signal conditioning

The sound produced by the animal is sensed with an electret microphone facing inward on his forehead. The electrical signal generated by the microphone is conditioned by an analog circuit that consists of three stages (Fig. 4).

In order to limit the signal bandwidth to the range of interest (below the cut-off frequency  $f_c=2$  kHz) and to minimize the effect of quantization

noise on the electrical signal, a low pass filter (low-pass filter 1 in Fig. 4) was designed and implemented. In order to obtain an output voltage lower than the corresponding to 1 least significant bit (LSB) at a  $f=f_c$ . It was required a minimum attenuation of 48.16 dB in the stopband. An eighth-order Butterworth low pass filter has been designed in a Sallen-Key configuration. The integrated circuit op-amp used for the filter implementation was a TLV2784 (Texas Instruments, Dallas, US).

An automatic gain control (AGC) amplifier MAX9814 (Maxim Integrated, San José, US) is used in order to maximize the signal-to-noise ratio (SNR), avoiding signal distortions, and clipping produced by high gain amplifications. The AGC output is connected to an analog input channel of the A/D converter in the MCU (*Analog input 0*), configured with 8 bits resolution. The number resulting from the conversion includes information of the sign of the signal. The AGC applied gain is available at an output pin, for supplying the MCU with this critical information through another input channel of the A/D converter (*Analog input 2*).

The AGC amplifier output is also connected to a second order Sallen-Key low pass filter (low-pass filter 2 in Fig. 4) with  $f_c=0.1\text{Hz}$  and unity gain. The op-amp used was an TLV2781 (Texas Instruments, Dallas, US). This filter computes the acoustic monitoring root mean square value, that it is both connected to a third input channel of then A/D converter in the MCU (*Analog input 1*) to detect when there is acoustic monitoring present and is compared with a defined threshold reference voltage using an TLV2781 in an op-amp voltage comparator configuration. The output compared signal is employed to wake-up the MCU (IRQ input) from the sleep mode.

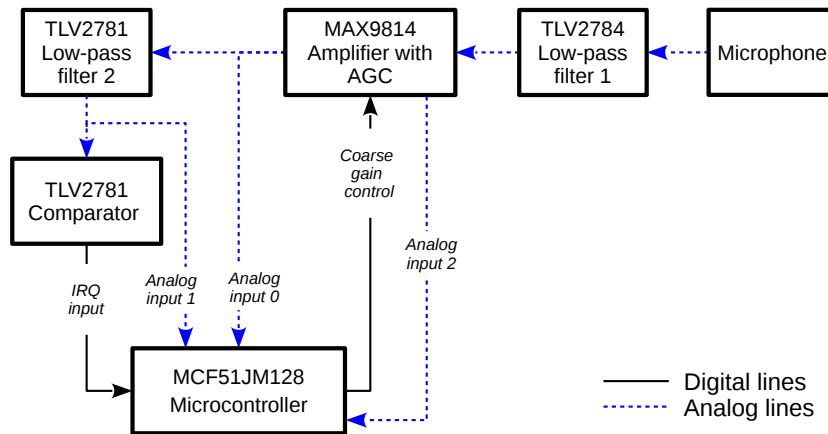


Figure 4: Block diagram of the signal conditioning circuit.

## 3.2 Digital Processing

The embedded software is organized in four tasks: *i*) signal conditioning and preprocessing, event detection, and classification, *ii*) data logging, *iii*) internal and external communication, and *iv*) device configuration. The software architecture is driven by interrupts that switch between active and sleep modes between interrupt events. The use of interrupt driven programming allows to the power consumption of the device to be optimized by using low power sleep modes ensuring a precise data sampling and processing intervals. Each of these four main interrupts wake up the MCU into active power mode and a routine is used to determine which function caused the interrupt event.

When the operational comparator detect an acoustic monitoring, the algorithm start to work for 5 min. Every 500  $\mu$ s time interval, the MCU goes to the active mode by the finished A/D conversion and then it execute the algorithm to detect and classify the ingestive events. Then, the software extract the information that characterized the ingestive activities and accumulates the partial results, and the MCU is set into sleep mode until the next finished A/D conversion. Finally, after 5 minutes since the last acoustic monitoring detection, the device is hibernated.

For every 15 min interval a data frame is built (Section 3.3), where the data frame is integrated by the information related to the feeding activities (i.e. quantity, average time, and average energy of each potential event), the time, and position at that moment. The time and position is obtained from a global positioning system (GPS) that normally operates in power save mode and it is switched to maximum performance mode to acquire the position. Finally, the data frame is stored as a text file in the flash memory, and the MCU is set into sleep mode.

Every 15 min the PC starts and control the wireless communication with the SUD, generating an interrupt in the MCU. It is achieved through the use of request and response packages protocol. The reception module of the transceiver is on continuously, waiting for a request package from the PC. When a request package is received, the MCU turns on the transmission module, transmits the requested data frames, waits for the reception acknowledgment of the PC and then it turns off the transmission module and the MCU.

The final interrupt routine is triggered by an Universal Serial Bus (USB) port data event. This is caused by messages being sent from the PC to the embedded system when an USB communication is established. When a download command is sent to the SUD, the MCU transfers the data stored in the flash memory to the PC through the USB port. A message containing a new configuration settings can also be sent to the SUD.

a) **##,D,T,Lat,Long,NC,DC,AC,EC,NB,DB,AB,EB,NCB,DCB,ACB,ECB,TNE,##**

Figure 5: Data file format used to store information

### 3.3 Data-logging and communications

Internal communications in the SUD are managed by the MCU, which collect  
190 data to create a data frame structure. The accurate time and position are  
obtained from a NEO-6M GPS receiver (u-blox,Thalwil, Suiza), using NMEA  
0183 standard to communicate with the microprocessor. A 3 V and 20mm  
CR2032 coin cell battery is incorporated as a backup power supply to ensure  
accurate time and position, as well as a fast startup of the GPS in the event  
195 of primary battery failure, since satellite ephemeris data and configuration  
settings are stored in the backup memory.

The data frame structure is created in the MCU, as shown in Fig. 5(a).  
It starts and ends with two numerals characters (#) and the data fields  
are separated by commas (.). This structure reduces the parsing time and  
200 avoids data loss or misleading. It has been categorized in two parts: *i*) the  
first four fields are the date (D), time (T), latitude (Lat), and longitude  
(Long) in NMEA 0183 standard format where the data was collected. *ii*)  
The remaining fields corresponds to the parameters of grazing activities. It  
stores the number of events (**C**, **B**, and **CB**), the average duration of time  
205 (DC, DB, and DCB), the average amplitude (AC, AB, and ACB), the average  
energy (EC, EB, and ECB) of the grazing events, respectively, and the the  
total number of events (TNE) . Each data field of this section is stored in  
32 bits integer format. This information is codified by using a low-density  
parity-check (LDPC) code to guarantee the integrity of the data from errors.

210 Data logging, time, and position stamping are carried out through the  
host MCU interfacing with two W25Q128FV serial flash-NOR memory chips  
(Winbond Electronics, Taichung, Taiwan).

The USB module provides an On-The-Go (OTG) dual-role controller.  
All these features simplify the hardware and software required for communi-  
215 cation. The additional wireless communication mode operating at 433/470  
MHz has been implemented using a UM402 SX1278 LoRa module (Man-  
Think Co., Beijing, China) with wired antenna that enables a transfer rate  
up to 37.5 kbps for a length range up to 6 km.

### 3.4 Power supply and energy harvesting

220 The design of a battery powered embedded system requires a detailed analysis of each subsystem and software to minimize power consumption, considering both energy provision and consumption simultaneously. In this way, the device has been designed with the goal of minimizing power consumption whereas it is able of harvest all the energy needed for its operation.

225 Therefore, three complementary approaches were used to develop the energy management scheme: *i*) A combined duty-cycling and data-driven operating scheme, driven by data, to operate only when relevant information is available. It is implemented through the embedded software in the micro-controller combined with an interrupt scheme to allow the digital parts of

230 the SUD to alternate between active and sleep modes, when there is acoustic monitoring present or not, respectively. *ii*) An energy harvesting scheme, by using a 1W solar panel (5.5 V open circuit voltage and 170 mA short circuit current) able to recharge the batteries when the SUD is operating outdoors; *iii*) A USB port when the device is connect to a PC or an energy source.

235 The duty-cycling power management scheme is implemented through the embedded software combined with the aforementioned interrupt scheme.

A high efficiency battery charge with protected overvoltage input and overcurrent input is provided between each harvester and the battery pack. These features enables the SUD to run with a defective or missing battery

240 pack. The battery power is supplied by two polymer batteries (Li-Ion 3.7 V 2500 mAh). The MCU monitors the true battery voltage through an analog input channel of the A/D converter (*Analog Input 3* in Fig. 6) and in case of errors, turn off the SUD to avoid problems in the detection and classification of events.

245 A primary regulated 3.3 V power supply is provided to the SUD through a high efficiency buck/boost charge pump regulator TPS63001 (Texas Instruments, Dallas, US). This integrated circuit allow to achieve a low ripple, stable high quality voltage, and long autonomy of the device.

## 4 Laboratory tests and discussion

250 To evaluate the performance of the proposed SUD, two experimental analysis have been performed. The first analysis is focused on the recognition and classification capabilities, whereas the second one lies on the power consumption and energy harvesting capabilities.

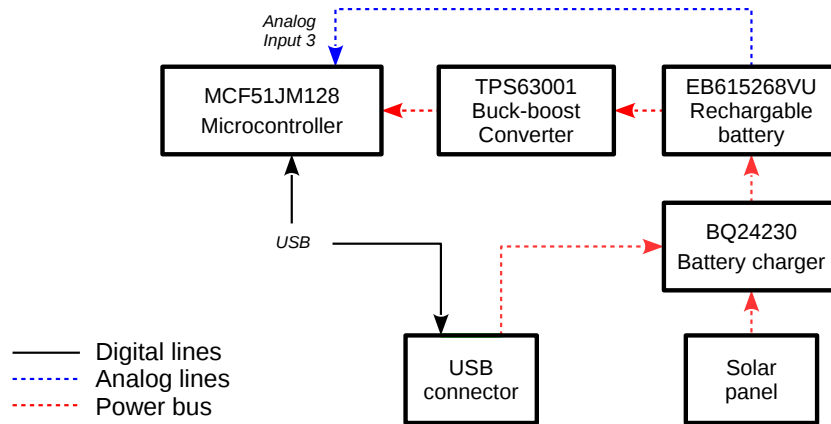


Figure 6: Block diagram of power supply circuit.

#### 4.1 Experimental Setup and Performance measurements

255 The validation of the system was done via laboratory tests. The soundtracks employed were obtained by a field experiment conducted at the Campo Experimental Villarino (Universidad Nacional de Rosario, Zavalla, Argentina) dairy facility, during october of 2014. The foraging behaviour of five Holstein lactating cows were continuously monitored during six non consecutive days.

260 The evaluation was performed with 24 hours continuous sound recordings at 44.1 kHz sampling frequency using 16-bit resolution and WAV format. The acoustic monitoring were recorded using a directional microphone mounted onto the forehead of the animal and covered by a elastic band fastened to a halter, where a commercial recorder was attached. The microphone/recorder

265 devices were randomly assigned to the cows and rotated over the six days.

For experiments, five representative segments of 10-min from a total of 24h of continuous audio recording were aurally segmented and labeled event by event within rumination and grazing activities by two experts in animal behaviour. In order to consider different types of foraging behaviours, each

270 segment consisted of 5-min of rumination (contain only chew events) and 5-min of grazing (contain the three types of events), which were randomly selected.

One important issue for the comparison between events recognized and classified by the algorithm and the corresponding reference labels made by

275 the experts is the synchronization time of events in both sequences. To solve this, the HTK performance analysis tool HResults was used. The comparison is based on a Dynamic Programming-based string alignment procedure [8]. The outputs of this tool were: (i) the number of deletions (D), which are considered as false negatives, (ii) the number of substitutions (S), which are

280 considered as misclassified events, (iii) the number of insertions (I), which are considered as false positives, and the total number of events (T) in the reference transcription files provided by the experts. Using this information, performance measures can be established. Regarding the **detection task**, the percentage of correctly detected events is defined as

$$D\% = (T - D)/T \ 100\% \quad (1)$$

285 where the number of substitutions was not considered, because it only matters if an event has occurred or not, regardless of the type of event. Regarding the **classification task**, the percentage number of labels correctly recognized **CL%** and the accuracy **A%** is given by

$$CL\% = (T - D - S)/T \ 100\% \quad (2)$$

$$A\% = (T - D - S - I)/T \ 100\% \quad (3)$$

290 where both substitutions S and insertions I are considered.

## 4.2 Recognition results

The main parameters used by Chelotti et. al (i.e. shape=2, intensity=0.3, duration=0.3s) suffer small adaptations due to the integer arithmetic used to achieve a real-time operation on the MCU. The recognition rates obtained from the analysis are shown in Table 1.

295 The results show that the embedded system developed was able to correctly detect and classify 78% of the feeding events. The best recognized event was the **C** event, in agreement with the results obtained by Chelotti et al. (2016)[6]. It should be noted the similarity between segment and for the average between the values of correct and accuracy, which evidences a low number of insertions (false positives) for the system, which represents a good stability of the proposed methodology. These results reveal that the analysis of the time-domain acoustic monitoring features shown properly the corresponding jaw motion. In addition it was shown that processing was executed in real-time.

## 4.3 Autonomy analysis

310 The estimation of the time in which the SUD will be in active mode is one of the most important parameters to know about the autonomy, because it is when the greatest energy consumption will occur. This time is the sum of the rumination and grazing activities, due to the fact that these are the periods in which the target masticatory events are present.

Table 1: Confusion matrix, average recognition rates and accuracy.

		Bite	Chew	Chew-bite	Correct	Accuracy
$S_1$	B	<b>82</b>	9	9		
	C	1	<b>98</b>	1	<b>78</b>	<b>77</b>
	CB	10	9	<b>81</b>		
$S_2$	B	<b>77</b>	8	15		
	C	1	<b>97</b>	2	<b>83</b>	<b>81</b>
	CB	5	6	<b>89</b>		
$S_3$	B	<b>81</b>	11	8		
	C	1	<b>97</b>	2	<b>75</b>	<b>74</b>
	CB	6	11	<b>83</b>		
$S_4$	B	<b>95</b>	5	0		
	C	4	<b>84</b>	12	<b>70</b>	<b>67</b>
	CB	3	11	<b>86</b>		
$S_5$	B	<b>84</b>	8	8		
	C	1	<b>96</b>	3	<b>85</b>	<b>83</b>
	CB	3	13	<b>84</b>		
Average					<b>78.2</b>	<b>76.4</b>

The circadian rhythm of the cattle feeding behaviour will be crucial to determine the SUD's autonomy. According to [9] during daylight hours, the average time of both activities (rumination and grazing) is about 40 min per hour, whereas during night this value drops to around 30 min. This indicates that the SUD will be in active mode around 60% of the daily time.

According to the values in Table 2, the calculated SUD current consumption during the active power mode is  $I_A = 34.9mA$ . The measured current consumption is 31-34 mA and it is close to the measured value. Every 5 min, due to the data frame interruption, the GPS is waked up and there is a peak consumption of 44 mA. When the SUD is in active mode, there are many current peaks of 34 mA each 500  $\mu s$ , which correspond to the sampling frequency of the acoustic monitoring signal and the execution of the detection and classification algorithm.

Taking into account the current consumption give by  $I_A$ , the charge consumption per hour during active mode will be 34.9 mAh. Considering a battery capacity of 5000 mAh (two batteries of 2500 mAh each) and in absence of the solar panel, the SUD would have an autonomy of  $T_A = 143.27h$ .

On the other hand, the instant measured current provided by the solar panel is 120 mA during daylight hours. If we suppose it is maintained during 6 h (25% of the daytime), the average charge provided per hour is  $Q_{SP} = 30.0mAh$ . According to the circadian cycle of the cattle feeding behaviour,

Table 2: Estimated power consumption and percentage duration of each module.

Module	Power Consumption [mA]	Time
MCU	11.5	100 %
Signal Conditioning	2.5	50 %
GPS	11.5	0.33 %
Communication RX/TX	13/110	5.00%/0.22%
Storage	4	0.33 %
Power Supply	20	100 %

the average charge consumed per hour for a whole day is given by  $Q_{CR} = 20.6mAh$ . Thus, the net charge balance is  $Q_{SP} - Q_{CR} = 9.4mAh$ . This shows that the harvested power is sufficient to energize the SUD.

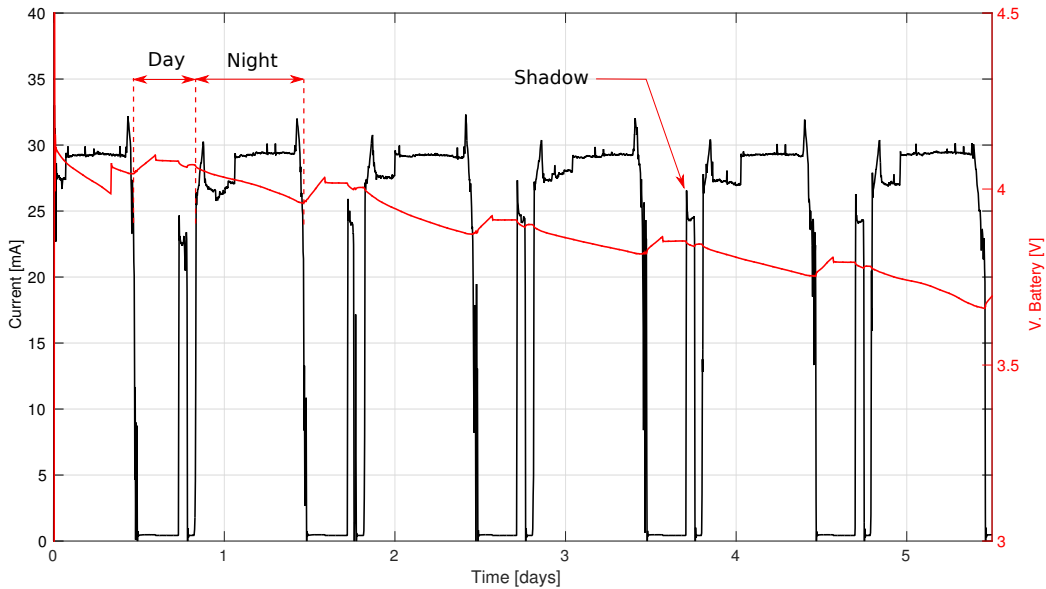


Figure 7: Current consumption (black line) and voltage of the battery pack (red line).

335

In order to determine the profile of voltage and current variations in the battery pack to estimate the autonomy of the SUD, it was tested in active power mode all the time, i.e., the worst-case conditions, during a period of 5 days outdoors with the batteries fully charged initially. In Fig. 7 the evolution of voltage and current of the batteries are shown. During the day, the current provided by the batteries decrease to zero, when the SUD is powered entirely by the solar panel and, at the same time, the batteries are partially recharged. However it is not enough to accomplish a full charge of the batteries. As

340

345 expected, during the night, the batteries supply the embedded system and  
its voltage decreases considerably. During each daylight, there is a small  
peak in the current consumption, which corresponds to the projection of a  
shadow above the solar panel making that much of the current consumed by  
the SUD has to be provided by the batteries during this time. This projected  
350 shadow emulates the situation in which there is no incident light on the solar  
panel during daylight, either by clouds covering the sun, by a motion of the  
cow's head, or because the cattle is located under a tree, among others.

At the end of the test, the SUD still worked properly and the voltage  
tends to stabilize close to 3.7 V, which is the nominal batteries voltage.

## 5 Conclusion

355 This paper introduces a novel embedded system for real-time monitoring the  
feeding behavior of ruminants by means of acoustic monitoring analysis. The  
motivation of this work was to provide a tool to enhance the understanding  
of feeding behavior of dairy cows by developing sensor technology that al-  
lows the continuous monitoring of animal feeding activities under different  
360 environmental conditions.

The proposed solution integrates different key technologies in a unique  
device, i.e. acoustic monitoring signal conditioning, wired/wireless commu-  
nications, data logging, power management, energy harvesting, and embed-  
ded detection and classification algorithm. The proposed methodology was  
365 implemented in a microcontroller and it is based on the analysis of certain  
characteristics of the acoustic monitoring signal, since the different jaw action  
of the animal have different shape, intensity, and duration.

The proposed embedded algorithm has been validated over a test bench  
by showing that it was able to correctly detect and classify 78% of the feeding  
370 events identified by human experts, which is similar to the results obtained  
by Chelotti et al. (2016)[6]. Regarding the power consumption, the sensor  
solution can work autonomously following the circadian rhythm of the cattle  
feeding behaviour, as well as, it can work for more than 5 days in the worst  
case, in which the animal feeds 24 hours a day, without recharging the bat-  
375 teries externally. When the solar panel is illuminated, it energizes the sensor  
and recharges the batteries.

Since the device has not yet been tested on animals, in future studies,  
the device will be tested on a cow under field operational conditions for  
380 continuous operation over time, where the cow motion and the weather could  
play important roles in the power supply system.

## References

- [1] A. Z. Abbasi, N. Islam, Z. A. Shaikh *et al.*, “A review of wireless sensors and networks’ applications in agriculture,” *Computer Standards & Interfaces*, vol. 36, no. 2, pp. 263–270, 2014.
- 385 [2] B. Panckhurst, P. Brown, K. Payne, and T. Molteno, “Solar-powered sensor for continuous monitoring of livestock position,” in *Sensors Applications Symposium (SAS), 2015 IEEE*. IEEE, 2015, pp. 1–6.
- [3] E. D. Ungar and S. M. Rutter, “Classifying cattle jaw movements: comparing iger behaviour recorder and acoustic techniques,” *Applied animal*  
390 *behaviour science*, vol. 98, no. 1, pp. 11–27, 2006.
- [4] J. R. Galli, C. A. Cangiano, D. H. Milone, and E. A. Laca, “Acoustic monitoring of short-term ingestive behavior and intake in grazing sheep,” *Livestock Science*, vol. 140, no. 1, pp. 32–41, 2011.
- [5] A. L. H. Andriamandroso, J. Bindelle, B. Mercatoris, F. Lebeau *et al.*,  
395 “A review on the use of sensors to monitor cattle jaw movements and behavior when grazing,” *BASE*, 2016.
- [6] J. O. Chelotti, S. R. Vanrell, D. H. Milone, S. A. Utsumi, J. R. Galli, H. L. Rufiner, and L. L. Giovanini, “A real-time algorithm for acoustic monitoring of ingestive behavior of grazing cattle,” *Computers and Electronics*  
400 *in Agriculture*, vol. 127, pp. 64–75, 2016.
- [7] D. H. Milone, J. R. Galli, C. A. Cangiano, H. L. Rufiner, and E. A. Laca, “Automatic recognition of ingestive sounds of cattle based on hidden markov models,” *Computers and electronics in agriculture*, vol. 87, pp. 51–55, 2012.
- 405 [8] S. Young, G. Evermann, M. Gales, T. Hain, D. Kershaw, X. Liu, G. Moore, J. Odell, D. Ollason, D. Povey *et al.*, “The htk book, vol. 2,” *Entropic Cambridge Research Laboratory Cambridge*, vol. 4, 1997.
- [9] L. Balocchi, F. Pulido, V. Fernández *et al.*, “Comportamiento de vacas lecheras en pastoreo con y sin suplementación con concentrado,” *Agricultura Técnica*, vol. 62, no. 1, pp. 87–98, 2002.
- 410